Submitted to JPCA, x/x/2019

Globally accurate full-dimensional potential energy surface for H_2 + HCl inelastic scattering

Qian Yao,[1] Masato Morita,[2] Changjian Xie,[1,#] Naduvalath Balakrishnan,[2,*] and Hua Guo[1,*]

[1]*Department of Chemistry and Chemical Biology, University of New Mexico, Albuquerque, New Mexico 87131, USA*

[2]*Department of Chemistry and Biochemistry, University of Nevada, Las Vegas, Nevada 89154, USA*

[#]: current address:

[*]: corresponding authors: naduvala@unlv.nevada.edu and hguo@unm.edu

Abstract

A globally accurate full-dimensional potential energy surface (PES) for the inelastic scattering between H_2 and HCl is developed based on a large number of points calculated at the coupled-cluster singles, doubles, and perturbative triples level of theory. The machine-learned PES is trained with xx such points using the permutation invariant polynomial-neural network method, resulting in a root mean square fitting error of xx cm^{-1}. Both full- and reduced-dimensional quantum calculations for the inelastic scattering are performed on this new PES and the agreement with the previous quantum dynamical results on a reduced-dimensional PES is excellent. Furthermore, strong resonances are identified at various collision energies, including cold conditions. This new PES provides a reliable platform for future studies of scattering dynamics with vibrationally excited collision partners.

I. Introduction

It has long established that all energies are not equal in collisional processes.[1-3] For reactive collisions, Polanyi observed that while translational energy is more effective in promoting a chemical reaction with an early barrier, vibrational energy enhances reactivity for a reaction with a late barrier.[4] Such mode specificity can also be viewed in the Sudden Vector Projection (SVP) model as the differing coupling strength of various reactant modes with the reaction coordinate at the transition state.[5] The SVP model has been shown to predict mode specificity in many systems involving polyatomic molecules.[6]

Experimental studies of mode specificity require the preparation of vibrational states. Until recently, this can only be achieved with a partial population of the desired vibrational levels, which complicates the analysis.[1, 2] More recently, laser based coherent techniques, such as stimulated emission pumping (SEP)[7] and adiabatic passage based method including Stimulated Raman Adiabatic Passage (STIRAP or SARP)[8] and Rapid Adiabatic Passage (RAP),[9] have enabled near 100% population of a specific ro-vibrational states in diatomic as well as polyatomic molecules. These new capabilities open new doors for studying the effects of internal energy on reactive and non-reactive collisional processes, which allow testing of new theory and models. In the latest experiment on the inelastic collision of SARP prepared excited HD(v=1) with H_2 in a co-expansion beam, for example, clear stereodynamical control was achieved at very low (~1 K) collision temperature.[10, 11]

Theoretically, the understanding of mode specificity requires the construction of the Born-Oppenheimer potential energy surface (PES) from the first principles and in full

dimensionality. This has been a great challenge,[12] but has recently been overcome, thanks to the advances in electronic structure theory and means to represent the PES using analytical functions.[13-18] With the PES, it is possible to calculate the dynamical attributes related to mode specificity, using either quantum mechanical or quasi-classical methods. In our recent investigation of Zare's SARP work on HD(v=1) + H_2 collisions,[10, 11] full-dimensional quantum scattering calculations were performed on the accurate PES of Hinde.[19] These highly accurate quantum dynamical calculations not only reproduced the experimentally observed stereodynamics, but also revealed the existence of dynamical resonances dominated by single partial waves.[20]

In the current work, we report the first full-dimensional PES for the H_2-HCl system. This system features a much stronger interaction than that between two H_2 molecules. Previous studies have identified two T-shape minima for the HCl–H_2 complex.[21-23] The global minimum corresponds to a T-shape geometry with the H atom of the HCl molecule pointing to the H_2 molecule and a secondary minimum has the Cl atom pointing to H_2. The PES is given in an analytical form based on a feed-forward neural network (NN), trained by xx points calculated with an explicitly correlated coupled cluster singles, doubles, and perturbative triples (CCSD(T)-F12b) level of theory. The permutation of the three hydrogens in this system is explicitly enforced using the permutation invariant polynomial-neural network (PIP-NN) method.[18] Using this new PES, full-dimensional calculations have been carried out using an exact time-dependent quantum scattering method with both molecules in their ground vibrational states, but with HCl in its first excited rotational state. Reduced-dimensional quantum scattering calculations have also been performed within the rigid rotor approximation.

The comparison of the two suggests that the rigid rotor approximation is quite accurate for inelastic scattering involving lowest lying states of the collision partners. In addition, the good agreement achieved with the previous reduced-dimensional quantum scattering results using a four-dimensional PES further validate the accuracy of the new full-dimensional PES. This new PES offers a reliable platform for future studies of inelastic scattering with internally excited H_2 and/or HCl molecules, which, along with other similar work, is expected to give accurate information on the vibrational effects on energy transfer.

II. Theory

II-A. *Ab initio* calculations

The geometry optimization for all stationary points and energies of all sampled points used for PES fitting were all calculated with the explicitly correlated (F12b) version of the coupled-cluster method with singles, doubles, and perturbative triples (CCSD(T)-F12b).[24] The augmented correlation-consistent polarized valence quadruple-zeta basis set (aug-cc-pVQZ or AVQZ)[25] was used. Since there is no bond breaking involved, this system can be reasonably described by a single reference method, as the T1 diagnostic value is typically below 0.008. The MOLPRO 2015.1 program package[26] was used in all *ab initio* calculations reported in this work.

The points in the training set were chosen according to the following recipe. First, stationary points were surveyed to determine the ranges of configurations and energies. Second, small grids with appropriate coordinates in various regions were used to sample relevant configurations. Then, the selected points are calculated at the CCSD(T)-F12b/AVQZ level and

a primitive PES was obtained by fitting the calculated *ab initio* points using the method detailed in the next subsection. Trajectories were launched with various initial conditions on the primitive PES to explore the configuration space and to generate new points. A new point ($\boldsymbol{r}$) was added if it is below an energy cutoff and satisfies the $\chi(r_i) = \sqrt{\sum_{i=1}^{6}|r_i - r_i'|^2} > 0.1$ Å condition for all points ($\boldsymbol{r}'$) in the training set. This process is repeated until convergence.

B. PES fitting

The PES is divided into two segments, namely the short-range and long-range parts. The short-range part of the PES, denoted as $V_{\text{PIP-NN}}$, was fit to *ab initio* points using the permutation invariant polynomial-neural network (PIP-NN) method.[18] A total of 42417 points below 2 eV relative to the global minimum on the PES were selected. In the PIP-NN approach, the input layer of the NN is given by low-order PIPs, rather than the internuclear distances (r_{ij}), which are invariant under inversion, but do not enforce the permutation symmetry. The invariance of the PES with respect to permutation of identical atoms is enforced by PIPs,[27, 28] which can be defined as symmetrized monomials:[13]

$$\boldsymbol{G} = \hat{S}\prod_{i<j}^{N} p_{ij}^{l_{ij}}, \quad (1)$$

where $\hat{S}$ is the symmetrization operator. N is the number of atoms. $p_{ij} = \exp(-r_{ij}/a)$ are Morse-like variables with a as an adjustable constant (a=1.5 Å) and l_{ij} is the order of the monomial.

In this work, the maximum order of the PIPs is 4, resulting in 50 terms in the input layer. In the NN fitting, a two-layer NN architecture, (N1-N2) = (20-80), with 2781 parameters was employed. Other numbers have been tested by they do not impact the results significantly. The

NN fittings were trained using the Levenberg-Marquardt algorithm with the root mean square error (RMSE) as the penalty function:

$$\mathrm{RMSE} = \sqrt{\sum_{i=1}^{N_{\mathrm{data}}} \frac{\left(E_{\mathrm{output}} - E_{\mathrm{target}}\right)^2}{N_{\mathrm{data}}}}, \tag{2}$$

where E_{output} and E_{target} are the fitted and input energies, respectively. In each NN training, the data were randomly divided into three sets, namely, the training (90% of the data points), validation (5%), and test (5%) sets. The training is terminated if the errors in the validation set starts to grow, thus avoiding overfitting. The test set is used to assess the quality of the NN fit in points that are not included in the training.

While the scattering is largely determined by PES in the short range, including the attractive and repulsive regions, the long-range interaction becomes important at low collision energies. For studies of cold and ultra-cold collisions, it is imperative to map out accurately the long-range PES. The long-range part of the PES, denoted as V_{LR}, is best expressed in the diatom-diatom Jacobi coordinates $(R, r_1, r_2, \theta_1, \theta_2, \varphi)$, which are defined in Figure 1. R is the distance between the centers of mass of H_2 and HCl, and r_1 and r_2 denote the bond lengths of H_2 and HCl, respectively. The polar angles of the H_2 and HCl molecules with respect to vector R are denoted by θ_1 and θ_2, respectively; and the dihedral angle is given by φ.

The long-range interaction employed the following expansion form:

$$V_{\mathrm{LR}}(R, r_1, r_2, \theta_1, \theta_2, \varphi) = V_{\mathrm{HCl}}(r_1) + V_{\mathrm{H_2}}(r_2) + V_{\mathrm{int}}(R, r_1, r_2, \theta_1, \theta_2, \varphi). \tag{3}$$

Here, V_{HCl} and $V_{\mathrm{H_2}}$ are the one-dimensional (1D) potential energy curves for isolated HCl and H_2 molecules, respectively. The V_{HCl} and $V_{\mathrm{H_2}}$ are spline-interpolated from *ab initio* data

points in the asymptote. V_{int} is the intermolecular interaction potential, which is the long-range interaction (R > 5 Å) between two molecular centers of mass and fitted by the linear least-squares method using the following expression,[29]

$$V_{\text{int}} = \sum_{l_1 l_2, m, n} C_{l_1 l_2, m, n} v_{l_1 l_2}(r_1, r_2) \frac{b_n^m(\theta_1, \theta_2, \varphi)}{R^n}. \quad (4)$$

A more detailed description of this formula and the choice of the parameters are given in the Supporting Information (SI). A total of 24870 *ab initio* points was used in the fitting and these points were selected from the 42417 ab initio points used in the PIP-NN fitting with R larger than 5 Å.

The overall PES is switched from the short-range PES to its long-range counterpart as R increases:

$$V_{\text{PES}} = sV_{\text{PIP-NN}} + (1 - s)V_{\text{LR}}, \quad (5)$$

where the switching function is defined as

$$s = \frac{1 - \tanh[3(R - 5.5\text{Å})]}{2}. \quad (6)$$

II-C. Quantum scattering calculations

III. Results

The ab initio well depth of the global minimum calculated in this work is 215.5 cm^{-1}, which is in good agreement with the previous theoretical value of 213.38 cm^{-1} reported by Lanza et al.[23] The well of the secondary minimum is just 3.5 cm^{-1} higher than the value of Lanza et al.[23] In Table I, the calculated geometries, energies, and harmonic frequencies for all

stationary points are listed.

The RMSEs of the three best PIP-NN fits for the training/validation/test sets and maximum deviation of the three best fits were 0.80/1.07/0.89/22.33 meV, 0.85/1.09/0.91/17.15 meV, 0.86/0.92/0.97/13.98 meV, respectively. The final PIP-NN PES was chosen as the average of three best fits and had an overall RMSE of 0.70 meV and a maximum deviation of 12.14 meV. As shown in Table 1, the fit values are in good agreement with the *ab initio* results obtained by using the CCSD(T)-F12b/AVQZ method. The energy difference is less than 7.1 cm^{-1} and the frequency difference is less than 24.8 cm^{-1}. In Figure 2, the PES is displayed with R and θ_2 when other four coordinates are fixed at xx values. The two T-shaped wells are clearly seen in the figure.

The fitting error of the long-range potential is xx cm-1. In Fig 3, *ab initio* data are compared with the PIP-NN PES, long-range PES and overall PES at different orientation. It can be readily seen that the long-range PES was in excellent agreement with the *ab initio* energies.

Supplementary Information: details of the long range interaction potential.

Acknowledgements: This work was supported by a MURI grant (xx) from ARO.

References

1. Crim, F. F. Vibrational state control of bimolecular reactions: Discovering and directing the chemistry, *Acc. Chem. Res.* **1999,** *32*, 877-884.
2. Liu, K. Vibrational control of bimolecular reactcions with methane with mode-, bond-, and stereo-selectivity, *Annu. Rev. Phys. Chem.* **2016,** *67*, 91-111.
3. Chadwick, H.; Beck, R. D. Quantum state–resolved studies of chemisorption reactions, *Annu. Rev. Phys. Chem.* **2017,** *68*, 39-61.
4. Polanyi, J. C. Concepts in reaction dynamics, *Acc. Chem. Res.* **1972,** *5*, 161-168.
5. Guo, H.; Jiang, B. The sudden vector projection model for reactivity: Mode specificity and bond selectivity made simple, *Acc. Chem. Res.* **2014,** *47*, 3679-3685.
6. Guo, H.; Liu, K. Control of chemical reactivity by transition state and beyond, *Chem. Sci.* **2016,** *7*, 3992-4003.
7. Silva, M.; Jongma, R.; Field, R. W.; Wodtke, A. M. The dynamics of "stretched molecules": experimental studies of highly vibrationally excited molecules with stimulated emission pumping, *Annu. Rev. Phys. Chem.* **2001,** *52*, 811.
8. Gaubatz, U.; Rudecki, P.; Schiemann, S.; Bergmann, K. Population transfer between molecular vibrational levels by stimulated Raman scattering with partially overlapping laser fields. A new concept and experimental results, *J. Chem. Phys.* **1990,** *92*, 5363-5376.
9. Chadwick, H.; Hundt, P. M.; van Reijzen, M. E.; Yoder, B. L.; Beck, R. D. Quantum state specific reactant preparation in a molecular beam by rapid adiabatic passage, *J. Chem. Phys.* **2014,** *140*, 034321.
10. Perreault, W. E.; Mukherjee, N.; Zare, R. N. Quantum control of molecular collisions at 1 kelvin, *Science* **2017,** *358*, 356-359.
11. Perreault, W. E.; Mukherjee, N.; Zare, R. N. Cold quantum-controlled rotationally inelastic scattering of HD with H_2 and D_2 reveals collisional partner reorientation, *Nat. Chem.* **2018,** *10*, 561-567.
12. Murrell, J. N.; Carter, S.; Farantos, S. C.; Huxley, P.; Varandas, A. J. C. *Molecular Potential Energy Functions*. Wiley: Chichester, 1984.
13. Braams, B. J.; Bowman, J. M. Permutationally invariant potential energy surfaces in high dimensionality, *Int. Rev. Phys. Chem.* **2009,** *28*, 577–606.
14. Czakó, G.; Bowman, J. M. Reaction dynamics of methane with F, O, Cl, and Br on ab initio potential energy surfaces, *J. Phys. Chem. A* **2014,** *118*, 2839–2864.
15. Li, J.; Jiang, B.; Song, H.; Ma, J.; Zhao, B.; Dawes, R.; Guo, H. From ab initio potential energy surfaces to state-resolved reactivities: The X + H_2O ↔ HX + OH (X=F, Cl, and O(^{3}P)) reactions, *J. Phys. Chem. A* **2015,** *119*, 4667-4687.
16. Behler, J. Constructing high-dimensional neural network potentials: A tutorial review, *Int. J. Quant. Chem.* **2015,** *115*, 1032-1050.
17. Dawes, R.; Ndengué, S. A. Single- and multireference electronic structure calculations for constructing potential energy surfaces, *Int. Rev. Phys. Chem.* **2016,** *35*, 441-478.
18. Jiang, B.; Li, J.; Guo, H. Potential energy surfaces from high fidelity fitting of ab initio points: The permutation invariant polynomial-neural network approach, *Int. Rev. Phys. Chem.* **2016,** *35*, 479-506.
19. Hinde, R. J. A six-dimensional H_2–H_2 potential energy surface for bound state

spectroscopy, *J. Chem. Phys.* **2008,** *128*, 154308.
20. Croft, J. F. E.; Balakrishnan, N.; Huang, M.; Guo, H. Unraveling the stereodynamics of cold controlled HD-H_2 collisions, *Phys. Rev. Lett.* **2018,** *121*, 113401.
21. Anderson, D. T.; Schuder, M.; Nesbitt, D. J. Large-amplitude motion in highly quantum clusters: high-resolution infrared absorption studies of jet-cooled H_2–HCl and H_2–DCl, *Chem. Phys.* **1998,** *239*, 253-269.
22. Alkorta, I.; Elguero, J.; Del Bene, J. E. An ab initio investigation of the properties of H_2:HX hydrogen-bonded complexes, *Chem. Phys. Lett.* **2010,** *489*, 159-163.
23. Lanza, M.; Kalugina, Y.; Wiesenfeld, L.; Lique, F. Near-resonant rotational energy transfer in HCl–H_2 inelastic collisions, *J. Chem. Phys.* **2014,** *140*, 064316.
24. Knizia, G.; Adler, T. B.; Werner, H.-J. Simplified CCSD(T)-F12 methods: Theory and benchmarks, *J. Chem. Phys.* **2009,** *130*, 054104.
25. Dunning, T. H. Gaussian basis sets for use in correlated molecular calculations. I. The atoms boron through neon and hydrogen, *J. Chem. Phys.* **1989,** *90*, 1007-1023.
26. Werner, H. J.; Knowles, P. J.; Knizia, G.; Manby, F. R.; Schütz, M. Molpro: a general-purpose quantum chemistry program package, *WIREs Comput. Mol. Sci.* **2012,** *2*, 242-253.
27. Jiang, B.; Guo, H. Permutation invariant polynomial neural network approach to fitting potential energy surfaces, *J. Chem. Phys.* **2013,** *139*, 054112.
28. Li, J.; Jiang, B.; Guo, H. Permutation invariant polynomial neural network approach to fitting potential energy surfaces. II. Four-atom systems, *J. Chem. Phys.* **2013,** *139*, 204103.
29. Buckingham, A. D. Permanent and induced molecular moments and long-range intermolecular forces, *Adv. Chem. Phys.* **1967,** *12*, 107-142.

Table 1. Energies (in cm^{-1}) and harmonic frequencies (in cm^{-1}) of the stationary points for the H_2 + HCl system.

species	level	energy	frequency					
			1	2	3	4	5	6
H_2+HCl	ab initio	215.5				4404.5		2992.0

	PES	216.9				4402.4		2991.8
$H_2\cdots HCl$	ab initio	0.0	97.3	122.0	141.6	334.6	2985.9	4387.3
	PES	0.0	99.3	118.6	137.5	320.8	2988.7	4388.7
$H_2\cdots ClH$	ab initio	112.9	61.7	90.7	102.2	150.0	2990.8	4400.2
	PES	120.0	72.5	89.3	102.1	125.2	2991.6	4397.2

Figure Captions

Fig. 1. Jacobi coordinates for the H_2–HCl system.

Fig. 2. Three-dimensional plot of the PES as a function of R and θ_2 with fixed r_1=0.74 Å, r_2=1.28 Å, θ_1=90 ˚ and φ=0 ˚. The two T-shaped minima are shown as potential wells.

Comparison of *ab initio* energies and the PIP-NN PES, long-range PES and overall PES at different orientation.

Fig. 4.

Fig.2

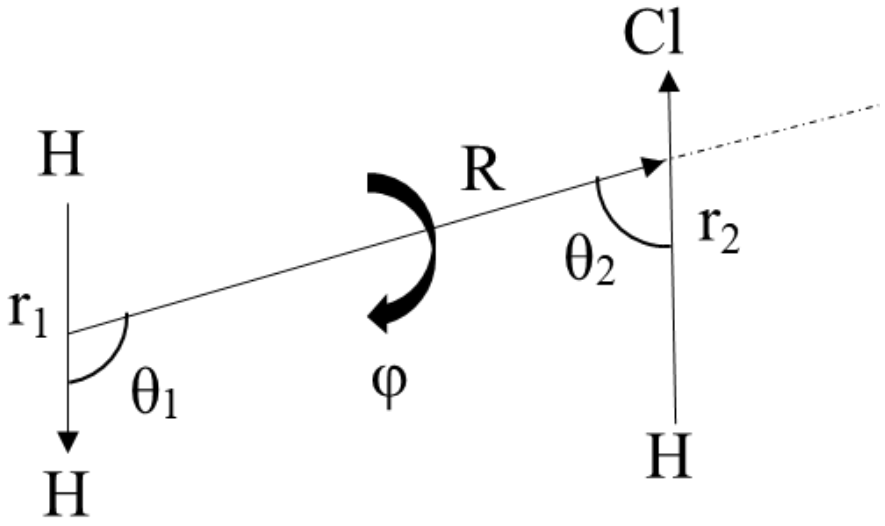

Fig.1

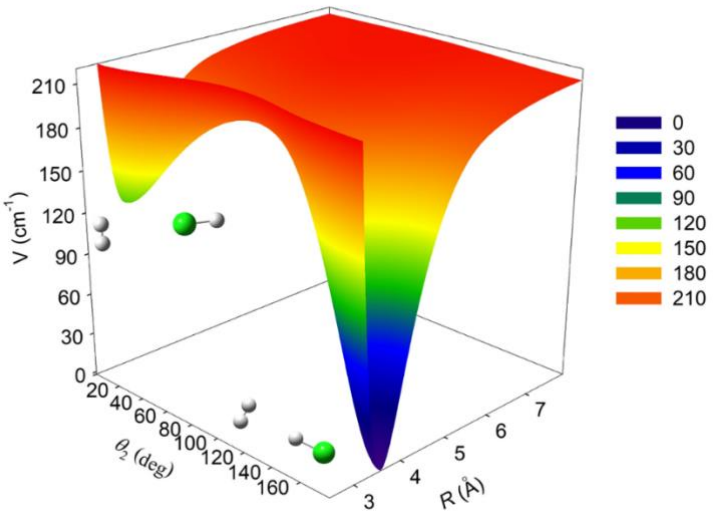
V (cm^{-1})
210
180
150
120
90
60
30
0
20
40
60
80
100
120
140
160
θ_2 (deg)
3
4
5
6
7
R (Å)
0
30
60
90
120
150
180
210

Fig.3

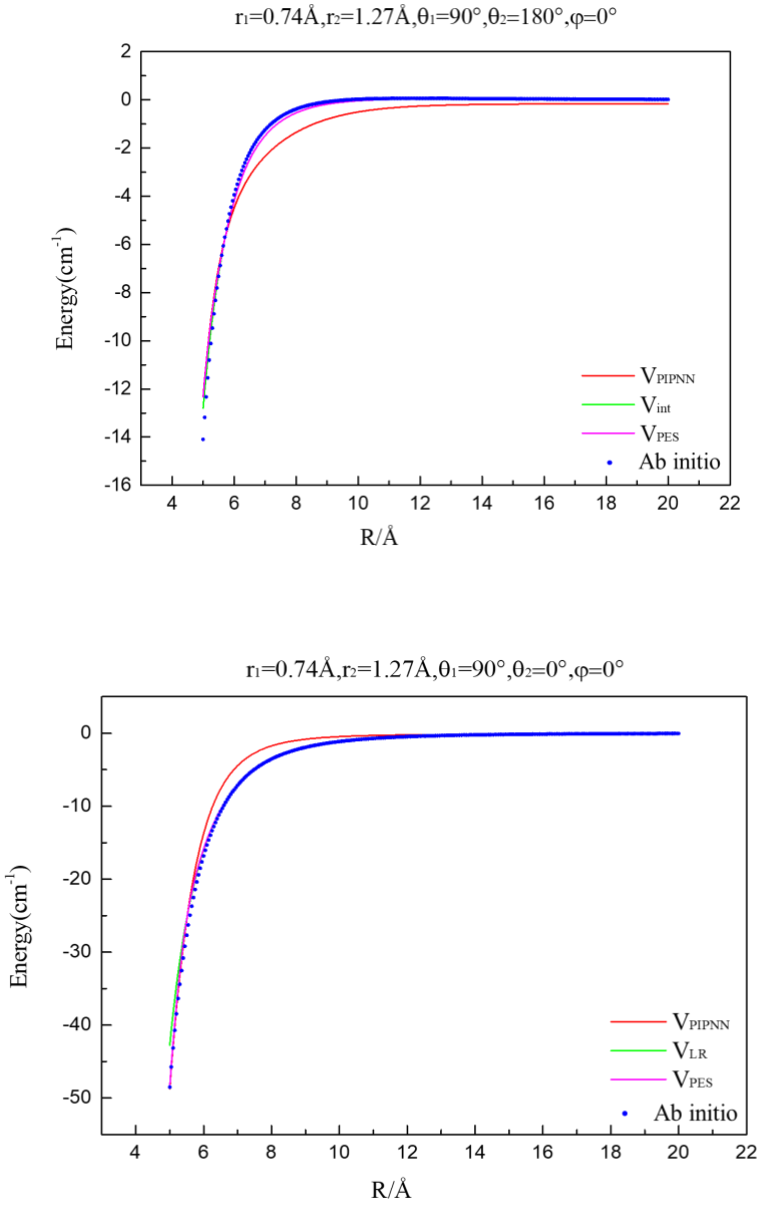
r1=0.74Å,r2=1.27Å,θ1=90°,θ2=180°,φ=0°
Energy(cm-1)
R/Å
VPIPNN
Vint
VPES
Ab initio
r1=0.74Å,r2=1.27Å,θ1=90°,θ2=0°,φ=0°
Energy(cm-1)
R/Å
VPIPNN
VLR
VPES
Ab initio

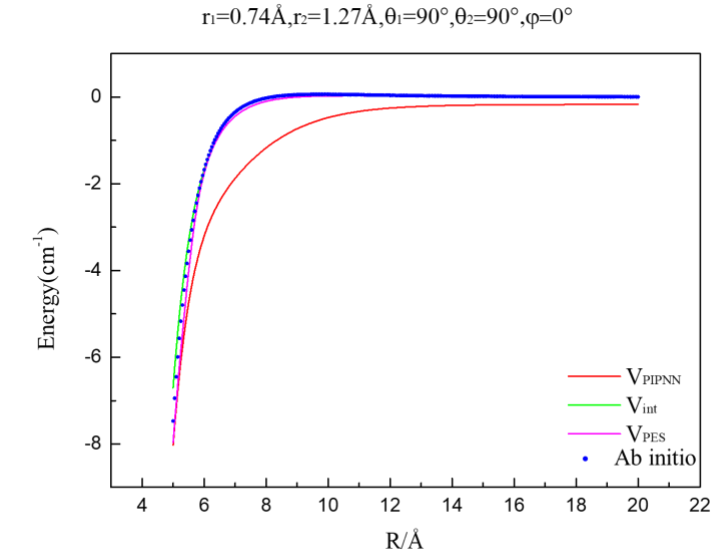
r1=0.74Å,r2=1.27Å,θ1=90°,θ2=90°,φ=0°
Energy(cm-1)
R/Å
VPIPNN
Vint
VPES
Ab initio

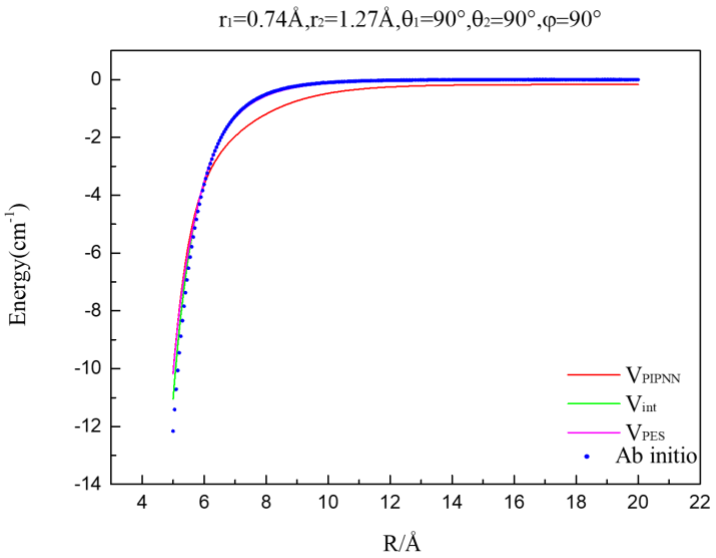
r1=0.74Å,r2=1.27Å,θ1=90°,θ2=90°,φ=90°
Energy(cm-1)
R/Å
VPIPNN
Vint
VPES
Ab initio

Fig.4

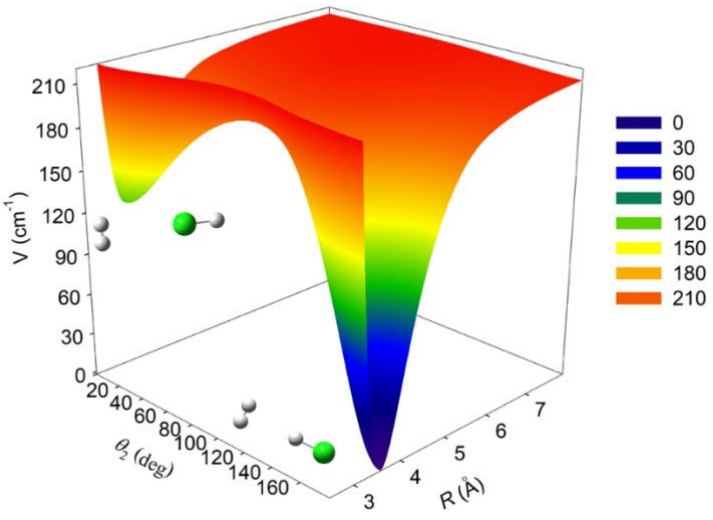
V (cm^{-1})
210
180
150
120
90
60
30
0
20
40
60
80
100
120
140
160
θ_2 (deg)
3
4
5
6
7
R (Å)
0
30
60
90
120
150
180
210